Published in final edited form as:

Mol Cancer Ther. 2016 August ; 15(8): 1879–1889. doi:10.1158/1535-7163.MCT-15-0335.

Macrophage-mediated trogocytosis leads to death of antibody-opsonized tumor cells

Ramraj Velmurugan[a,b,c], **Dilip K. Challa**[a,b,c], **Sripad Ram**[d], **Raimund J. Ober**[a,e,*], and **E. Sally Ward**[a,b,*]

[a]Department of Molecular and Cellular Medicine, College of Medicine, Texas A&M Health Science Center, College Station, TX 77843, USA

[b]Department of Microbial Pathogenesis and Immunology, Texas A&M Health Science Center, Bryan, TX 77807, USA

[c]Biomedical Engineering Graduate Program, University of Texas Southwestern Medical Center, 5323 Harry Hines Boulevard, Dallas, TX 75390, USA

[e]Department of Biomedical Engineering, Texas A&M University, College Station, TX 77843, USA

Abstract

Understanding the complex behavior of effector cells such as monocytes or macrophages in regulating cancerous growth is of central importance for cancer immunotherapy. Earlier studies using CD20-specific antibodies have demonstrated that the Fcγ receptor (FcγR)-mediated transfer of the targeted receptors from tumor cells to these effector cells through trogocytosis can enable escape from antibody therapy, leading to the viewpoint that this process is pro-tumorigenic. In the current study we demonstrate that persistent trogocytic attack results in the killing of HER2-overexpressing breast cancer cells. Further, antibody engineering to increase FcγR interactions enhances this tumoricidal activity. These studies extend the complex repertoire of activities of macrophages to trogocytic-mediated cell death of HER2-overexpressing target cells and have implications for the development of effective antibody-based therapies.

Keywords

Trogocytosis; antibody therapy; macrophages; phagocytosis; antibody engineering

Introduction

Defining the consequences of the interactions of immune effector cells with cancer cells in the presence of tumor-specific antibodies has direct relevance to both immunosurveillance and cancer therapy. The effects of therapeutic antibodies can include the direct inhibition of cell signaling through growth factor receptor binding and the indirect consequences of tumor

*Corresponding authors: Raimund J. Ober, Department of Biomedical Engineering, Texas A&M University, College Station, TX 77843, USA; email, raimund.ober@tamu.edu; E. Sally Ward, Department of Molecular and Cellular Medicine, College of Medicine, Texas A&M Health Science Center, College Station, TX 77843, USA; email, sally.ward@medicine.tamhsc.edu.

[d]Current address: Pfizer, Inc., 10646 Science Center Drive, San Diego, CA 92121, USA.

Conflicts of interest: No potential conflicts of interest declared.

cell opsonization and recruitment of effector cells such as macrophages or natural killer (NK) cells (1). For example, monocytes or macrophages can interact with antibody-opsonized tumor cells and engulf whole cells or internalize fragments of the target cell plasma membrane during phagocytosis or trogocytosis, respectively (2-7). Although the tumoricidal effects of phagocytosis are clear, the effect of trogocytosis is less certain. It has been speculated that trogocytosis can have a positive effect during cancer therapy (6). Conversely, trogocytosis can result in escape from antibody-dependent cell-mediated cytotoxicity (ADCC), complement-dependent cytotoxicity (CDC) or phagocytic cell death. This mechanism of escape has been extensively studied for anti-CD20 antibodies (2, 3, 8, 9) and involves the depletion of target antigen from the cell surface combined with the exhaustion of effector pathways. These observations have led to the development of dosing regimens to reduce trogocytosis and minimize the pro-tumorigenic effects during CD20 targeting (10). However, in different settings it remains possible that trogocytosis results in tumor cell death. To date, such analyses have been limited by the challenges in distinguishing trogocytosis from phagocytosis in effector:target cell co-cultures. In the current study we have developed an assay to distinguish these two processes. This assay has been used to investigate whether trogocytosis leads to the attrition of HER2-overexpressing breast cancer cells. Establishment of trogocytosis as a pathway for tumor cell death has implications for strategies to optimize antibody-based therapies.

The involvement of FcγR-expressing effector cells in anti-tumor effects has motivated the use of antibody engineering approaches directed toward the Fc region to enhance FcγR binding affinity (11-16). However, due to the challenges associated with quantitating trogocytosis, how Fc engineering affects this activity is unexplored. In addition, despite the expansion in the development and use of antibody-based therapeutics during the past decade (17, 18), the factors leading to the induction of long-lived anti-tumor immunity are ill-defined. Consequently, understanding the mechanisms through which macrophages interact with tumor cells is not only important for Fc engineering, but also has relevance to elucidating the subcellular trafficking processes resulting in antigen acquisition and presentation by this antigen presenting cell subset (19, 20).

In the current study, we have used a novel approach to investigate the ability of macrophages of different sources to carry out trogocytosis and phagocytosis of antibody-opsonized HER2-overexpressing breast cancer cells. The RAW264.7 macrophage cell line very rarely phagocytoses complete cells, but has trogocytic activity similar to that of other macrophage types. Combined with analyses of apoptotic markers on opsonized target cells in the presence of both human and mouse macrophages, this behavior has allowed us to demonstrate that trogocytosis can lead to tumor cell death. Using multifocal plane microscopy (MUM) to image dynamic processes in three dimensions within cells (21, 22), we have also analyzed the spatiotemporal aspects of trogocytosis in live cells. We observe that this process involves the extension of opsonized tubules that are subsequently pinched off by the macrophage to form internalized trogocytic compartments. Of direct relevance to Fc engineering, the enhancement of antibody affinity for FcγRs results in increased trogocytosis and target cell death. Importantly, this higher activity is only manifested in the presence of physiological levels of intravenous gammaglobulin (IVIG). Collectively, these

studies indicate that trogocytosis can have tumoricidal effects that are further enhanced by antibody engineering.

Materials and Methods

Cell lines and primary cells

The murine macrophage cell lines RAW264.7 and J774A.1, the human breast cancer cell lines MDA-MB-453, SK-BR-3 were purchased from the American Type Culture Collection (ATCC). The HCC1954 cell line was a gift from Drs. Adi Gazdar, John Minna and Kenneth Huffman, UT Southwestern Medical Center, Dallas. The cell lines were maintained in the following media supplemented with 10% fetal calf serum (FCS; Gemini Bio-products): macrophages, phenol red-free Dulbecco's Modified Eagle Medium (DMEM); MDA-MB-453, RPMI-1640; SK-BR-3, McCoy's. HCC1954 cells were maintained in RPMI-1640 with 5% FCS. All experiments were conducted in medium containing FCS depleted of immunoglobulin G (IgG; 23), with the exception of experiments using Fc-engineered antibodies. Identities of all cancer cell lines were authenticated by short tandem repeat analysis on October 9, 2015 (University of Arizona Genetics Core). Murine macrophage cell lines purchased from the ATCC were maintained for less than 6 months in the laboratory. Purified human monocytes were purchased as frozen cells (Astarte Biologics) or purified from peripheral blood mononuclear cells (PBMCs, kindly provided by Darrell Pilling, Texas A&M University) using the EasySep Human Monocyte Enrichment Kit (Stemcell Technologies). The monocytes were cultured in DMEM containing 10% FBS supplemented with 50 ng/ml M-CSF (Peprotech) in 48 well plates, MatTek dishes or T25 flasks for six days prior to use in assays. Purified primary human B cells were purchased as frozen cells (Astarte Biologics), thawed according to the manufacturer's protocols and used in experiments within 24 hours.

Antibodies

Clinical-grade trastuzumab, pertuzumab, rituximab and intravenous gammaglobulin (IVIG; Gamunex) were obtained from the UT Southwestern Pharmacy. Monovalent Fab fragments derived from pertuzumab were generated using a Pierce Fab Preparation Kit (Thermo Scientific). Trastuzumab, rituximab, pertuzumab and pertuzumab Fab fragments were labeled using Alexa 488 or 555 labeling kits (Life Technologies). The construction of trastuzumab heavy and light chain expression constructs was performed as described previously (24). Mutations to enhance the binding of trastuzumab (human IgG1) to FcγRs, G236A/I332E (AE) and G236A/S239D/I332E (ADE; 13) were introduced into the trastuzumab expression construct by splicing by overlap extension (25). Sequences of expression constructs are available upon request. Wild type (WT) and mutated trastuzumab were expressed in transfected CHO cells using previously described methods (24). Pharmacy grade trastuzumab was used in all assays with the exception of the comparison of WT trastuzumab and AE/ADE variants. Antibodies specific for mouse FcγRs (clone X54-5/7.1 for FcγRI, 93 for FcγRII/III and 9E9 for FcγRIV) and the corresponding isotype controls were purchased from Biolegend.

Isolation of thioglycollate-elicited macrophages

C57BL/6J mice (purchased from The Jackson Laboratory) or human FcγR-transgenic C57BL/6J mice (gift from Dr. Jeffrey Ravetch, The Rockefeller University) (26) were housed in a pathogen-free animal facility at UT Southwestern Medical Center or the Texas A&M Health Science Center and handled according to protocols approved by the Institutional Animal Care and Use Committees. 8-12 week old male mice were intraperitoneally injected with 3 ml aged thioglycollate (gift from Dr. Chandrashekar Pasare, UT Southwestern Medical Center). After 72 hours, the mice were sacrificed and peritoneal macrophages isolated by peritoneal lavage. The macrophages were plated in the assay plates in complete DMEM containing 10% FCS, and assays were performed 1-3 days later using the same conditions as for the macrophage cell lines.

Analyses of macrophage effects on tumor cell numbers

Target cells were harvested, labeled with carboxyfluorescein succinimidyl ester (CFSE; Life Technologies) and mixed with effector cells at the indicated effector:target ratios in wells of 48-well plates, centrifuged to obtain an even distribution in the wells and allowed to attach overnight. Cells were treated with 1 μg/ml trastuzumab and incubated at 37°C for 72 hours. The cells were harvested by trypsinization, incubated with PerCP-labeled anti-mouse CD45 antibody (clone 30-F11, BD Biosciences) and Alexa 488-labeled pertuzumab, washed and fixed with formalin. For human macrophage effectors, anti-human CD45 antibody (HI30, Biolegend) was used to identify macrophages. A constant number of Flow Check 6 μm high-intensity yellow-green beads (PolySciences, Inc.) were added to each tube and the samples analyzed by flow cytometry (BD FACSCalibur or LSR Fortessa). The number of cancer cells in each sample was calculated by counting the CFSE-positive events, followed by normalization with the bead counts.

For the analysis of staining of tumor cells by annexin V and propidium iodide (PI), co-cultures were incubated as above for 36 hours. Harvested cells were stained with Alexa 647-labeled annexin V and PI (Life Technologies) or BV421-labeled annexin V (BD Biosciences), followed by quantitation of the fraction of annexin V-positive, PI-positive, CD45-negative cells using flow cytometry. For the analysis of caspase activity in the tumor cells, the co-cultures were treated with 2 μM CellEvent Caspase-3/7 Green Detection Reagent (Life Technologies) for the last four hours of incubation.

Whole cell phagocytosis assay

Effector cells were plated in 24 well plates, centrifuged to ensure an even distribution and incubated for 18 hours. Six hours prior to addition of target cells and opsonizing antibody, cells were treated with 25 ng/ml IFN-γ. Target cells were incubated with 5 μM 5-ethynyl-2′-deoxyuridine (EdU) provided with the Click iT EdU Flow Cytometry Kit (Life Technologies) for 48 hours prior to the assay, harvested by trypsinization, added at the appropriate effector:target ratios and incubated at 37°C for 3-6 hours in the presence of 1 μg/ml trastuzumab. The cells were harvested, treated with 10 μg/ml human IgG1 to block non-specific binding and incubated with 3 μg/ml PerCP-labeled anti-mouse CD45 antibody and 10 μg/ml Alexa 488-labeled pertuzumab for ten minutes on ice. The cells were subsequently washed, resuspended in 50% formalin in PBS and stained for EdU using the

EdU flow cytometry kit protocol. Samples were analyzed using flow cytometry (BD FACSCalibur or LSR Fortessa). Percentage whole cell phagocytosis (WCP) was calculated as the fraction of EdU+ cells that were also CD45-positive and pertuzumab-negative.

Statistics

Tests for statistical significance between groups were carried out using Student's *t*-test or one-way ANOVA with Tukey's multiple comparisons test in GraphPad Prism (GraphPad Software). *p*-values of less than 0.05 were considered significant.

Results

Quantitation of cancer cell killing by macrophages

We initially analyzed the effects of different macrophage cells on the viability of opsonized, HER2-overexpressing breast cancer cells. The co-culture of J774A.1 or RAW264.7 macrophages with MDA-MB-453 or SK-BR-3 cells in the presence of the anti-HER2 antibody, trastuzumab, resulted in ∼90% and ∼50% decreases in target cell numbers, respectively (Fig. 1A,B). The efficiency of tumor cell recovery was similar for all co-culture conditions, excluding the possibility that variability in cell harvesting efficiency contributes to the differences in cell numbers (Fig. S1). Incubation of target cells with trastuzumab alone resulted in ∼ 10-20% reduction in cell numbers within 72 hours, consistent with earlier studies (27) (Fig. 1C), although larger decreases (∼50%) were observed following longer incubation times (24). The significant reductions in cell numbers within 72 hours (Fig. 1A,B) are therefore due to the presence of macrophages rather than the cytostatic effects of trastuzumab. Similar results were obtained for co-cultures maintained in growth media recommended for either the macrophage or tumor cell lines (Figs. 1, S2). To investigate whether the death of opsonized target cells in the presence of macrophages was due to the release of soluble mediators, cancer cells were cultured for 72 hours in the lower chambers of transwell plates containing macrophage:target cell co-cultures plus trastuzumab in the upper chambers (Fig. S3). The results demonstrate that macrophage:cancer cell contact is necessary for cell number attrition. In addition, treatment of cultures with an inhibitor of oxygen radical generation, edaravone, did not reduce cell death (Fig. S4).

The different levels of cell killing induced by incubation of trastuzumab-opsonized cancer cells with J774A.1 or RAW264.7 macrophages prompted us to use fluorescence microscopy to investigate the interactions between these effector:target cell combinations. Co-incubation of J774A.1 macrophages and MDA-MB-453 cells in the presence of trastuzumab led to the appearance of both phagocytosed cancer cells (whole cell phagocytosis, WCP) and cancer cell fragments, or trogosomes, within the CD45-positive macrophages (Fig. 2A, Movie S1). Permeabilization of the cells prior to staining with anti-mouse CD45 antibody demonstrated that the phagosomes and trogosomes have associated CD45, indicating that they were encapsulated by the macrophage plasma membrane (Fig. 2B). Similar observations were made using SK-BR-3 and HCC1954 cells as targets (Fig. S5A). By marked contrast, although RAW264.7 cells were active in trogocytosis, phagocytic events involving complete cells were not observed when these macrophages and trastuzumab-opsonized breast cancer cells (MDA-MB-453, SK-BR-3 or HCC1954) were co-cultured (no WCP events were

observed in 21 fields of view for RAW264.7 cells whereas 12/31 fields of view contained WCP events for J774A.1 macrophages; Fig. S5B). Consistent with the earlier observations of others (13, 28, 29), the use of human monocyte-derived macrophages as effectors with trastuzumab-opsonized tumor cells resulted in both trogocytosis and phagocytosis, combined with a decrease in cancer cell numbers (Fig. S6).

Trogocytosis leads to tumor cell death

To quantitate trogocytosis and WCP in a high throughput manner, we developed a flow cytometric assay involving the labeling of the DNA of tumor cells with EdU (Fig. 2C,D). To distinguish macrophage-associated tumor cells that were phagocytosed from those that formed macrophage:cancer cell couples, we reasoned that phagocytosed cells would be inaccessible to the anti-HER2 antibody, pertuzumab (30). Importantly, we and others have demonstrated that pertuzumab does not compete with trastuzumab for binding and can therefore be used to detect HER2 in the presence of trastuzumab (31-33). To quantitate cancer cells that had not been phagocytosed, co-cultures were harvested and stained with labeled pertuzumab, whereas EdU staining was used to identify all cancer cells. WCP activity was quantitated by determining the fraction of EdU-positive cells that were mouse CD45- positive and pertuzumab-negative, whereas cell couples were positive for all three markers. In the absence of trastuzumab, for J774.1 macrophages the number of cell couples was higher than in the presence of this antibody (Fig. 2C), most likely because cell couples formed with antibody-opsonized cancer cells are expected to lead to efficient target cell phagocytosis. The CD45-negative, pertuzumab-low population represents cancer cells that have substantially reduced surface HER2 levels due to trogocytosis.

We first used the flow cytometric assay to characterize the dynamics of WCP in J774A.1:MDA-MB-453 co-cultures. Using an effector:target cell ratio of 10:1, approximately 25% of the target cells were phagocytosed within 3 hours. This number increased over time, reaching a plateau level of 40-50% following 8 hours (Fig. 2E). WCP events are detectable even when the numbers of macrophages and cancer cells are equivalent or cancer cells outnumber the macrophages (effector:target ratios of 1:1 or 1:5), although the fraction of cancer cells that undergo WCP decreases (Fig. S7).

Thioglycollate-elicited primary peritoneal mouse macrophages and human monocyte-derived macrophages exhibited similar phagocytic activity to that observed for J774A.1 cells (Fig. 2F, S6C). Concordant with the microscopy data, RAW264.7 cells rarely performed WCP (Fig. 2F), whereas trogocytic activity was similar for all macrophage cell types (Fig. 2G). Analogous results were obtained for phagocytosis using SK-BR-3, HCC1954 or MDA-MB-453 cells as targets, demonstrating that the low phagocytic activity of RAW264.7 macrophages is not target cell-dependent (Fig. 2H,I). The percentage recovery of cancer cells for cell co-cultures with mouse and human macrophages were similar (70 – 80%; Fig. S1), excluding the possibility that differential recovery contributes to the observed differences in phagocytic activity between macrophage:cancer cell combinations.

The relatively high level of tumor cell death in the presence of RAW264.7 cells (Fig. 1B) combined with the very low levels of WCP activity indicated that trogocytosis can lead to tumor cell killing. To further investigate this, we performed long-term imaging of J774A.

1:SK-BR-3 or RAW264.7:SK-BR-3 co-cultures (at a 4:1 effector:target ratio) in the presence of trastuzumab for approximately 3 days. In agreement with the fixed cell and flow cytometry data, multiple phagocytic events involving whole cells were observed for J774A.1 macrophages, whereas WCP rarely occurred for RAW264.7 macrophages. Individual cancer cells undergoing trogocytosis by both J774A.1 and RAW264.7 macrophages could be observed, and in multiple cases cancer cell death was observed following several days of intermittent trogocytic attack (Movie S2 for J774A.1, Fig. 3A and Movie S3 for RAW264.7 macrophages; data shown are representative of at least 14 events observed for each macrophage type). Similar trogocytic attack followed by cell death was observed when human macrophages were used as effectors (Movie S4).

Live cell fluorescence microscopy also demonstrated that the non-phagocytic interactions between macrophages and cancer cells involved the transfer of trastuzumab from cancer cells to macrophages via trogocytosis (Movie S5). CellEvent Caspase 3/7 Green Detection Reagent was not detectable in the opsonized target cells during the early stages of trogocytic attack (within 3 hours of co-culture set up; Movie S5), indicating that the macrophages accumulate trogosomes from live cells during this time frame. However, following 36 hours of co-culture incubation of opsonized tumor cells with J774A.1, RAW264.7 and human monocyte-derived macrophages, ∼10% of target cells were positive for propidium iodide (PI) and fluorescently labeled annexin V (Fig. 3B,C,D, S8A,B). The annexin V-positive cells also accumulated CellEvent Caspase-3/7 Green Detection Reagent, indicating the induction of apoptosis (Fig. S8A). The percentages of PI/annexin V-positive cells are lower than those for the cumulative cell death following 72 hours incubation (Fig. 1), since PI/annexin V staining identifies a specific phase on the cell death pathway. In addition, surface HER2 levels were reduced on all of the opsonized cancer cells in the presence of macrophages (Fig. 3B,E,F). Combined with the survival of a proportion of cancer cells following 72 hours co-culture with macrophages (Fig. 1), this indicates that not all trogocytosed cells undergo cell death within this time frame. Nevertheless, in combination with our live cell imaging experiments and the observation that soluble mediators do not contribute to macrophage (RAW264.7)-mediated death of opsonized targets, these data demonstrate that trogocytosis can lead to tumor cell attrition.

Trogocytosis involves tubular extensions of opsonized cancer cells

We employed live cell imaging to study the uptake of labeled trastuzumab from the cancer cell surface into the macrophage. Macrophages accumulate punctate, trastuzumab-positive trogocytic compartments, resulting in depletion of trastuzumab from the cancer cell surface in the region adjacent to the macrophage (Fig. 4A). Following trastuzumab depletion, antibody levels in the region between the apposed cells recover within about 10 minutes, indicating that HER2/trastuzumab complexes are mobile on the cell surface. We next used MUM (21, 22) combined with live cell imaging to analyze the dynamics of trogocytosis in three dimensions (Fig. 4B,C). MUM enables the simultaneous visualization of cellular trafficking processes in multiple different focal planes (21, 34). Using MUM, we observed that trogocytosis involves the extension of tubular structures from the tumor cells into invaginations in the macrophage that are subsequently pinched off to form trogosomes within the effector cells (Fig. 4B,C, Movie S6). Flow cytometry analyses indicated that

although the levels of surface HER2 decrease on the target cells (Fig. 4D), the CFSE fluorescence level does not change following two days of co-incubation with macrophages in the presence of trastuzumab (Fig. 4E), indicating the engulfment of tubular extensions with high surface area:volume ratios. In addition, following two hours of incubation of macrophages with tumor cells, many trastuzumab-positive trogosomes are located in lysosomes (Fig. S9).

Although RAW264.7 cells rarely performed WCP, fluorescence microscopy indicated that the cell contacts with opsonized tumor cells were similar for both J774A.1 and RAW264.7 cells with respect to membrane ruffling and accumulation of actin and mouse CD45 (Fig. S10). In addition, both cell lines express all of the mouse FcγRs (Fig. S11). Interestingly, we did not observe capping of HER2 at the interface between cancer cells and macrophages or in cancer cells incubated with antibody only (Figs. S10, S12A). By contrast, in the presence of the anti-CD20 antibody, rituximab, capping of CD20 occurred on the surface of B cells isolated from human peripheral blood mononuclear cells (PBMCs; Fig. S12B), consistent with earlier observations (35-38). Further, following 30 or 60 minutes incubation, rituximab was more rapidly depleted from B cells compared with the reduction of trastuzumab associated with MDA-MB-453 breast cancer cells (Fig. S12C).

FcγR affinity enhancement modulates the levels of trastuzumab-mediated trogocytosis

The engineering of antibodies to selectively enhance their affinity for binding to activating FcγRs over inhibitory FcγRs provides a pathway for improving antibody efficacy *in vivo* (11-16). However, it is unknown whether this enhancement affects trogocytosis. We therefore analyzed the effects of two sets of mutations, G236A/I332E (AE) and G236A/S239D/I332E (ADE), on trogocytic activity. These mutations selectively increase the affinity of IgG1 for FcγRIIa or FcγRIIIa over the inhibitory receptor, FcγRIIb, resulting in higher 'Activatory/Inhibitory ratios' (13, 39). In addition, the ADE mutations result in higher affinity interactions with FcγRs than the AE mutations (13). Thioglycollate-elicited peritoneal macrophages isolated from transgenic mice that express human FcγRs, but not mouse FcγRs (26), were used for these experiments. Trogocytosis of cancer cells opsonized with wild type trastuzumab or FcγR-enhanced variants of this antibody was analyzed using a flow cytometric assay that quantitates the amount of labeled pertuzumab-Fab fragment associated with macrophages. To distinguish cancer cell:macrophage conjugates from macrophages that had trogocytosed material derived from cancer cells, we used an antibody specific for the cancer cell marker EpCAM in the absence of cell permeabilization.

Although the AE mutant displayed higher trogocytic efficiency than the WT antibody, the ADE mutant did not lead to an enhancement of trogocytosis over WT trastuzumab (Fig. 5A). Further, quantitation of WCP demonstrated that the addition of trastuzumab harboring AE or ADE mutations did not result in increased WCP activity following 3-6 hours incubation (Figs. 5B, S13). These results prompted us to explore the effects of the mutations in the presence of high concentrations of endogenous IgG to mimic *in vivo* conditions. In the presence of 10 mg/ml IVIG, addition of trastuzumab harboring AE and ADE mutations resulted in substantially increased trogocytic activity over the almost background levels observed with WT trastuzumab (Fig. 5C). These low levels of trogocytic activity of WT

antibodies in the presence of competing IgG are consistent with the observations of others (40). Interestingly, the WCP activities were significantly decreased by the addition of IVIG for both WT trastuzumab and the mutated variants (Fig. 5B,D). Similar inhibitory effects were observed when polyclonal, non-aggregated IgGs were purified from IVIG (Fig. S14), indicating that aggregated IgG does not contribute to this activity of IVIG. To investigate the consequences of IVIG addition on tumor cell death, cancer cell numbers were quantitated following 5 days co-incubation with WT trastuzumab or AE/ADE variants in the presence of macrophages and 10 mg/ml IVIG (Fig. 5E). The results demonstrate that the ADE variant is significantly more active than WT trastuzumab in reducing cancer cell numbers in the presence of macrophages, whereas the cytostatic effects of the antibodies alone on the cancer cells were similar for WT trastuzumab and the AE/ADE variants (Fig. 5E). Comparison of the effects of WT trastuzumab and the ADE variant in the presence of human monocyte-derived macrophages and IVIG on target cell death also demonstrated increased tumoricidal activity of the FcγR-enhanced mutant (Fig. S15). Consistent with the low level of trogocytic and phagocytic activity of WT trastuzumab in the presence of competing IVIG, our observations indicate that the cytostatic effect of trastuzumab is the major contributor to the target cell death induced by this antibody (Figs. 5E, S15). Collectively, these observations demonstrate that although the effector mechanisms of the macrophages have been significantly impaired by IVIG, their tumoricidal effects in the presence of trastuzumab can be increased by FcγR-enhancement.

Discussion

In the current study we demonstrate that macrophage-mediated trogocytosis can lead to relatively efficient death of antibody-opsonized breast cancer cells, with around 50% reduction in target cell numbers over a period of three days. Consequently, cancer cells are able to sustain limited membrane damage, but they are not resistant to persistent trogocytosis over extended periods. A possibility that is not mutually exclusive is that the depletion of HER2 from the plasma membrane ablates growth factor-mediated signaling in HER2-addicted cells, resulting in cell death (6). Interestingly, in earlier studies trogocytosis has been shown to efficiently remove target receptors such as CD20 from the plasma membrane, leading to amelioration of the tumoricidal effects of NK cells and macrophages in the presence of antibodies such as rituximab (8, 9). Macrophages can have both tumor promoting or inhibitory effects (41, 42), and our observations extend this dichotomous behavior to trogocytosis.

By contrast with the induction of clustering of lymphocyte receptors at the effector:target cell interface in the presence of opsonizing antibodies such as rituximab (35-38), we do not observe trastuzumab capping on cancer cells. In addition, during live cell imaging, following the trogocytic removal of fluorescently-labeled trastuzumab from the closely apposed target cell membrane, trastuzumab redistributes to the interface within around 10 minutes. This indicates that trastuzumab-HER2 complexes are mobile in the plasma membrane. The difference in receptor clustering suggests that the proportion of targeted receptor over other membrane constituents is lower in trogosomes derived from breast cancer cells. In addition, capping of receptors followed by their rapid removal from rituximab-opsonized lymphocytes is expected to not only reduce NK cell- and complement-mediated target cell death, but also

limit the duration of trogocytosis (40). This is consistent with the observation that trogocytosis of rituximab-CD20 complexes on CD20-expressing EL4 cells does not lead to therapeutic effects in tumor-bearing mice (9) and can result in tumor escape during CD20-targeted therapy (43). Consequently, the dynamic behavior of the opsonized antigen on the target cell surface is expected to modulate tumor cell killing by trogocytosis.

Recent studies in mouse models have demonstrated that Kupffer cells phagocytose antibody-opsonized circulating tumor cells (CTCs), leading to reductions in metastatic lesions (4). By contrast, in the absence of tumor-specific antibody, trogocytosis rather than WCP of CTCs was observed which did not lead to tumor cell death. The apparent discrepancy between our study and these earlier analyses is most likely due to the limited contact time between CTCs and macrophages in the absence of antibody, although we cannot exclude a contribution of the difference in target (4). In the current study, tumor cell death is observed when the target cells are adhered to the substratum and remain in contact with trogocytic macrophages for prolonged periods. This setting might more closely resemble macrophage-mediated attack on solid tumors rather than CTCs. Specifically, the physical constraints of surrounding cells in solid tumors are expected to favor trogocytosis over phagocytosis.

The contribution of trogocytosis to tumor cell death in the current study has been elucidated through our observation that WCP of several different cancer cells is very rarely observed when using RAW264.7 macrophages as effector cells. The behavior of RAW264.7 cells is consistent with the observations of others (6), and has been suggested to be due to the large size of the target cells. However, our observations that RAW264.7 cells rarely phagocytose three different breast tumor cell lines, combined with the relatively efficient phagocytic engulfment of these cell lines by J774A.1 macrophages, indicates that there are intrinsic properties of RAW264.7 cells restricting their ability to perform WCP. This could relate to differences in cytoskeletal organization or differentiation state. In this context, actin and CD45 accumulation at the macrophage:cancer cell interface did not indicate differences between RAW264.7 and J774A.1 macrophages when analyzed by fluorescence microscopy. However, by contrast with our observations and those of others (6), it was recently reported that RAW264.7 cells phagocytose trastuzumab-opsonized BT-474 cells (44). Further studies are required to determine the reasons for this apparent discrepancy.

Our microscopy studies of the spatiotemporal aspects of trogocytosis indicate that this process involves the engulfment of tubules extending from the target cell membrane rather than vesicular structures. These tubules are subsequently pinched off to form trogosomes within the macrophage. The involvement of tubular extensions, which can in multiple cases only be visualized using MUM due to their three dimensional, highly dynamic nature, is consistent with the accumulation of high levels of plasma membrane relative to the cytosolic contents of the target cell. This also has implications for antigen presentation by trogocytic macrophages, since it would bias toward the delivery of plasma membrane-associated proteins over cytosolic proteins to the intracellular, degradative compartments that represent the sites of antigen loading onto MHC class II molecules (45).

Our studies also have direct relevance to the affinity enhancement of antibodies for FcγRs (11-16). In the absence of competing IgG, we observe that the AE mutations, but not the

ADE mutations, confer increased trogocytic activity. Further, WCP was not affected by either of the mutation sets. In the absence of IVIG, it is possible that increased activity due to affinity/avidity enhancement is obscured through the WT antibody/FcγR interactions already being at maximal levels under the conditions of these assays. By contrast, in the presence of competing IVIG both AE and ADE mutations significantly increase macrophage-mediated trogocytosis, and to a lesser extent, phagocytosis. This translates to greater reductions in cancer cell viability for cells opsonized with trastuzumab-ADE compared with WT trastuzumab. In agreement with the observations of others (14), this reinforces the importance of performing such assays in the presence of endogenous antibody to ensure that the observations are physiologically relevant.

Several functions have been proposed for trogocytosis (46). For example, it can lead to the acquisition of antigen in the form of peptide-MHC complexes by T cells followed by their fratricide (47). In addition, trogocytosis has been suggested to provide a conduit for cell-cell transfer of materials (48-50). These studies and our current observations indicate that cells are tolerant to limited amounts of trogocytosis. This leads to the speculation that this process represents a tolerizing mechanism for self-antigens that is important for normal physiology. Consequently, the binding of autoreactive antibodies to cells may lead to trogocytic uptake by antigen presenting cells and immunological tolerance. Under these conditions, target cell death would be detrimental. By contrast, for tumor targeting with therapeutic antibodies, the relatively high antibody load could convert low level ‘background’ trogocytosis into an active tumoricidal effect.

Collectively, our studies have resulted in novel insight into the spatiotemporal dynamics and consequences of macrophage-mediated trogocytosis. Importantly, we demonstrate that this process involves the engulfment of tubular extensions and can lead to substantial attrition of tumor cells. Further, FcγR affinity enhancement results in significant increases in trogocytic activity. These observations extend the anti-tumor effects of macrophages to trogocytosis and have implications for the design of efficacious therapeutic antibodies.

Supplementary Material

Refer to Web version on PubMed Central for supplementary material.

Acknowledgments

We thank Dr. Jeffrey V. Ravetch (Rockefeller University, New York) for generously providing the human FcγR mice. We are indebted to Drs. Adi Gazdar, John Minna and Kenneth Huffman (UT Southwestern Medical Center, Dallas) for generously providing HCC1954 cells and to Dr. Raghava Sharma for assistance with isolating thioglycollate-elicited macrophages. We thank the UTSW Flow Cytometry Core for providing flow cytometry services and the UT Southwestern Live Cell Imaging Core for use of their Deltavision microscope. We thank Darrell Pilling (Texas A&M University) for providing PBMC samples. We would also like to thank Dr. Zhuo Gan for assistance with microscopy experiments, and J. Bregg Reedy for help with plasmid generation and CHO cell transfections.

Grant support: This research was supported in part by grants from the Cancer Prevention and Research Institute of Texas (RP110069, awarded to R. J. Ober and RP110441, awarded to E. S. Ward and R. J. Ober) and the National Institutes of Health (RO1GM85575, awarded to R. J. Ober).

References

1. Adams GP, Weiner LM. Monoclonal antibody therapy of cancer. Nat Biotechnol. 2005; 23:1147–57. [PubMed: 16151408]
2. Williams ME, Densmore JJ, Pawluczkowycz AW, Beum PV, Kennedy AD, Lindorfer MA, et al. Thrice-weekly low-dose rituximab decreases CD20 loss via shaving and promotes enhanced targeting in chronic lymphocytic leukemia. J Immunol. 2006; 177:7435–43. [PubMed: 17082663]
3. Daubeuf S, Lindorfer MA, Taylor RP, Joly E, Hudrisier D. The direction of plasma membrane exchange between lymphocytes and accessory cells by trogocytosis is influenced by the nature of the accessory cell. J Immunol. 2010; 184:1897–908. [PubMed: 20089699]
4. Gul N, Babes L, Siegmund K, Korthouwer R, Bogels M, Braster R, et al. Macrophages eliminate circulating tumor cells after monoclonal antibody therapy. J Clin Invest. 2014; 124:812–23. [PubMed: 24430180]
5. Chao MP, Alizadeh AA, Tang C, Myklebust JH, Varghese B, Gill S, et al. Anti-CD47 antibody synergizes with rituximab to promote phagocytosis and eradicate non-Hodgkin lymphoma. Cell. 2010; 142:699–713. [PubMed: 20813259]
6. Pham T, Mero P, Booth JW. Dynamics of macrophage trogocytosis of rituximab-coated B cells. PLoS One. 2011; 6:e14498. [PubMed: 21264210]
7. Montalvao F, Garcia Z, Celli S, Breart B, Deguine J, Van Rooijen N, et al. The mechanism of anti-CD20-mediated B cell depletion revealed by intravital imaging. J Clin Invest. 2013; 123:5098–103. [PubMed: 24177426]
8. Beum PV, Peek EM, Lindorfer MA, Beurskens FJ, Engelberts PJ, Parren PW, et al. Loss of CD20 and bound CD20 antibody from opsonized B cells occurs more rapidly because of trogocytosis mediated by Fc receptor-expressing effector cells than direct internalization by the B cells. J Immunol. 2011; 187:3438–47. [PubMed: 21841127]
9. Boross P, Jansen JH, Pastula A, van der Poel CE, Leusen JH. Both activating and inhibitory Fcγ receptors mediate rituximab-induced trogocytosis of CD20 in mice. Immunol Lett. 2012; 143:44–52. [PubMed: 22285696]
10. Taylor RP, Lindorfer MA. Fcγ-receptor-mediated trogocytosis impacts mAb-based therapies: historical precedence and recent developments. Blood. 2015; 125:762–6. [PubMed: 25498911]
11. Stavenhagen JB, Gorlatov S, Tuaillon N, Rankin CT, Li H, Burke S, et al. Fc optimization of therapeutic antibodies enhances their ability to kill tumor cells in vitro and controls tumor expansion in vivo via low-affinity activating Fcγ receptors. Cancer Res. 2007; 67:8882–90. [PubMed: 17875730]
12. Desjarlais JR, Lazar GA, Zhukovsky EA, Chu SY. Optimizing engagement of the immune system by anti-tumor antibodies: an engineer's perspective. Drug Discov Today. 2007; 12:898–910. [PubMed: 17993407]
13. Richards JO, Karki S, Lazar GA, Chen H, Dang W, Desjarlais JR. Optimization of antibody binding to FcγRIIa enhances macrophage phagocytosis of tumor cells. Mol Cancer Ther. 2008; 7:2517–27. [PubMed: 18723496]
14. Herter S, Birk MC, Klein C, Gerdes C, Umana P, Bacac M. Glycoengineering of therapeutic antibodies enhances monocyte/macrophage-mediated phagocytosis and cytotoxicity. J Immunol. 2014; 192:2252–60. [PubMed: 24489098]
15. Jung ST, Kelton W, Kang TH, Ng DT, Andersen JT, Sandlie I, et al. Effective phagocytosis of low Her2 tumor cell lines with engineered, aglycosylated IgG displaying high FcγRIIa affinity and selectivity. ACS Chem Biol. 2013; 8:368–75. [PubMed: 23030766]
16. Herter S, Herting F, Mundigl O, Waldhauer I, Weinzierl T, Fauti T, et al. Preclinical activity of the type II CD20 antibody GA101 (obinutuzumab) compared with rituximab and ofatumumab in vitro and in xenograft models. Mol Cancer Ther. 2013; 12:2031–42. [PubMed: 23873847]
17. Hogarth PM, Pietersz GA. Fc receptor-targeted therapies for the treatment of inflammation, cancer and beyond. Nat Rev Drug Discov. 2012; 11:311–31. [PubMed: 22460124]
18. Scott AM, Wolchok JD, Old LJ. Antibody therapy of cancer. Nat Rev Cancer. 2012; 12:278–87. [PubMed: 22437872]

19. Trombetta ES, Mellman I. Cell biology of antigen processing in vitro and in vivo. Annu Rev Immunol. 2005; 23:975–1028. [PubMed: 15771591]
20. Tseng D, Volkmer JP, Willingham SB, Contreras-Trujillo H, Fathman JW, Fernhoff NB, et al. Anti-CD47 antibody-mediated phagocytosis of cancer by macrophages primes an effective antitumor T-cell response. Proc Natl Acad Sci USA. 2013; 110:11103–8. [PubMed: 23690610]
21. Prabhat P, Gan Z, Chao J, Ram S, Vaccaro C, Gibbons S, et al. Elucidation of intracellular recycling pathways leading to exocytosis of the Fc receptor, FcRn, by using multifocal plane microscopy. Proc Natl Acad Sci USA. 2007; 104:5889–94. [PubMed: 17384151]
22. Prabhat P, Ram S, Ward ES, Ober RJ. Simultaneous imaging of different focal planes in fluorescence microscopy for the study of cellular dynamics in three dimensions. IEEE Trans Nanobioscience. 2004; 3:237–42. [PubMed: 15631134]
23. Ober RJ, Martinez C, Vaccaro C, Zhou J, Ward ES. Visualizing the site and dynamics of IgG salvage by the MHC class I-related receptor, FcRn. J Immunol. 2004; 172:2021–9. [PubMed: 14764666]
24. Kang JC, Poovassery JS, Bansal P, You S, Manjarres IM, Ober RJ, et al. Engineering multivalent antibodies to target heregulin-induced HER3 signaling in breast cancer cells. MAbs. 2014; 6:340–453. [PubMed: 24492289]
25. Horton RM, Hunt HD, Ho SN, Pullen JK, Pease LR. Engineering hybrid genes without the use of restriction enzymes: gene splicing by overlap extension. Gene. 1989; 77:61–8. [PubMed: 2744488]
26. Smith P, DiLillo DJ, Bournazos S, Li F, Ravetch JV. Mouse model recapitulating human Fcγ receptor structural and functional diversity. Proc Natl Acad Sci USA. 2012; 109:6181–6. [PubMed: 22474370]
27. Cretella D, Saccani F, Quaini F, Frati C, Lagrasta C, Bonelli M, et al. Trastuzumab emtansine is active on HER-2 overexpressing NSCLC cell lines and overcomes gefitinib resistance. Mol Cancer. 2014; 13:143. [PubMed: 24898067]
28. Leidi M, Gotti E, Bologna L, Miranda E, Rimoldi M, Sica A, et al. M2 macrophages phagocytose rituximab-opsonized leukemic targets more efficiently than m1 cells in vitro. J Immunol. 2009; 182:4415–22. [PubMed: 19299742]
29. Lefebvre ML, Krause SW, Salcedo M, Nardin A. Ex vivo-activated human macrophages kill chronic lymphocytic leukemia cells in the presence of rituximab: mechanism of antibody-dependent cellular cytotoxicity and impact of human serum. J Immunother. 2006; 29:388–97. [PubMed: 16799334]
30. Agus DB, Akita RW, Fox WD, Lewis GD, Higgins B, Pisacane PI, et al. Targeting ligand-activated ErbB2 signaling inhibits breast and prostate tumor growth. Cancer Cell. 2002; 2:127–37. [PubMed: 12204533]
31. Ram S, Kim D, Ober RJ, Ward ES. The level of HER2 expression is a predictor of antibody-HER2 trafficking behavior in cancer cells. MAbs. 2014; 6:1211–9. [PubMed: 25517306]
32. Franklin MC, Carey KD, Vajdos FF, Leahy DJ, de Vos AM, Sliwkowski MX. Insights into ErbB signaling from the structure of the ErbB2-pertuzumab complex. Cancer Cell. 2004; 5:317–28. [PubMed: 15093539]
33. Cho HS, Mason K, Ramyar KX, Stanley AM, Gabelli SB, Denney DW Jr, et al. Structure of the extracellular region of HER2 alone and in complex with the Herceptin Fab. Nature. 2003; 421:756–60. [PubMed: 12610629]
34. Ram S, Kim D, Ober RJ, Ward ES. 3D single molecule tracking with multifocal plane microscopy reveals rapid intercellular transferrin transport at epithelial cell barriers. Biophys J. 2012; 103:1594–603. [PubMed: 23062352]
35. Griffin FM Jr, Griffin JA, Silverstein SC. Studies on the mechanism of phagocytosis. II. The interaction of macrophages with anti-immunoglobulin IgG-coated bone marrow-derived lymphocytes. J Exp Med. 1976; 144:788–809. [PubMed: 1085341]
36. Michel RB, Mattes MJ. Intracellular accumulation of the anti-CD20 antibody 1F5 in B-lymphoma cells. Clin Cancer Res. 2002; 8:2701–13. [PubMed: 12171904]

37. Rudnicka D, Oszmiana A, Finch DK, Strickland I, Schofield DJ, Lowe DC, et al. Rituximab causes a polarization of B cells that augments its therapeutic function in NK-cell-mediated antibody-dependent cellular cytotoxicity. Blood. 2013; 121:4694–702. [PubMed: 23613524]
38. Taylor RB, Duffus WP, Raff MC, de Petris S. Redistribution and pinocytosis of lymphocyte surface immunoglobulin molecules induced by anti-immunoglobulin antibody. Nat New Biol. 1971; 233:225–9. [PubMed: 20480991]
39. Nimmerjahn F, Ravetch JV. Divergent immunoglobulin G subclass activity through selective Fc receptor binding. Science. 2005; 310:1510–2. [PubMed: 16322460]
40. Beum PV, Lindorfer MA, Taylor RP. Within peripheral blood mononuclear cells, antibody-dependent cellular cytotoxicity of rituximab-opsonized Daudi cells is promoted by NK cells and inhibited by monocytes due to shaving. J Immunol. 2008; 181:2916–24. [PubMed: 18684983]
41. Grugan KD, McCabe FL, Kinder M, Greenplate AR, Harman BC, Ekert JE, et al. Tumor-associated macrophages promote invasion while retaining Fc-dependent anti-tumor function. J Immunol. 2012; 189:5457–66. [PubMed: 23105143]
42. Qian BZ, Pollard JW. Macrophage diversity enhances tumor progression and metastasis. Cell. 2010; 141:39–51. [PubMed: 20371344]
43. Taylor RP, Lindorfer MA. Analyses of CD20 monoclonal antibody-mediated tumor cell killing mechanisms: rational design of dosing strategies. Mol Pharmacol. 2014; 86:485–91. [PubMed: 24944188]
44. Shi Y, Fan X, Deng H, Brezski RJ, Rycyzyn M, Jordan RE, et al. Trastuzumab triggers phagocytic killing of high HER2 cancer cells in vitro and in vivo by interaction with fcγ receptors on macrophages. J Immunol. 2015; 194:4379–86. [PubMed: 25795760]
45. Blum JS, Wearsch PA, Cresswell P. Pathways of antigen processing. Annu Rev Immunol. 2013; 31:443–73. [PubMed: 23298205]
46. Joly E, Hudrisier D. What is trogocytosis and what is its purpose? Nat Immunol. 2003; 4:815. [PubMed: 12942076]
47. Nakamura K, Nakayama M, Kawano M, Amagai R, Ishii T, Harigae H, et al. Fratricide of natural killer cells dressed with tumor-derived NKG2D ligand. Proc Natl Acad Sci USA. 2013; 110:9421–6. [PubMed: 23690625]
48. Huang JF, Yang Y, Sepulveda H, Shi W, Hwang I, Peterson PA, et al. TCR-mediated internalization of peptide-MHC complexes acquired by T cells. Science. 1999; 286:952–4. [PubMed: 10542149]
49. Ahmed KA, Munegowda MA, Xie Y, Xiang J. Intercellular trogocytosis plays an important role in modulation of immune responses. Cell Mol Immunol. 2008; 5:261–9. [PubMed: 18761813]
50. Davis DM. Mechanisms and functions for the duration of intercellular contacts made by lymphocytes. Nat Rev Immunol. 2009; 9:543–55. [PubMed: 19609264]

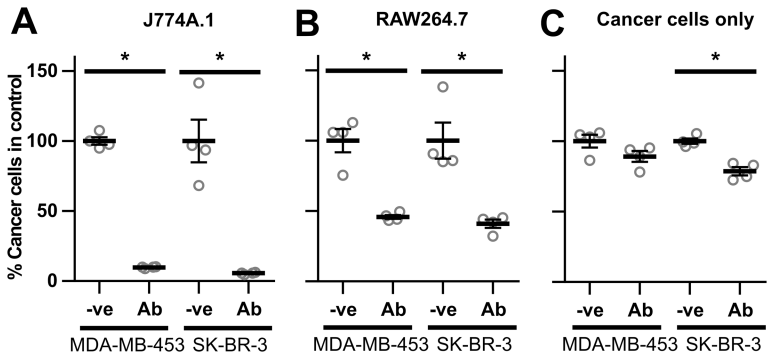

Figure 1.

Macrophages reduce breast cancer cell viability in the presence of trastuzumab. J774A.1 (**A**) or RAW264.7 (**B**) macrophages were plated in 48 well plates with MDA-MB-453 or SK-BR-3 breast cancer cells at a 4:1 effector:target cell ratio (2.5×10^4:6.25×10^3 cells) and 1 μg/ml trastuzumab (Ab) or PBS vehicle (-ve) was added 24 hours later. Following 72 hours, cells were harvested and the remaining number of cancer cells quantitated by flow cytometry. The number of live cancer cells in each sample is shown as a fraction of the corresponding vehicle control. **C**, cell numbers following incubation of cancer cells as in **A,B** but without macrophages. Error bars represent standard errors. Student's *t*-test was performed to indicate statistical significance (denoted by *; $p < 0.05$).

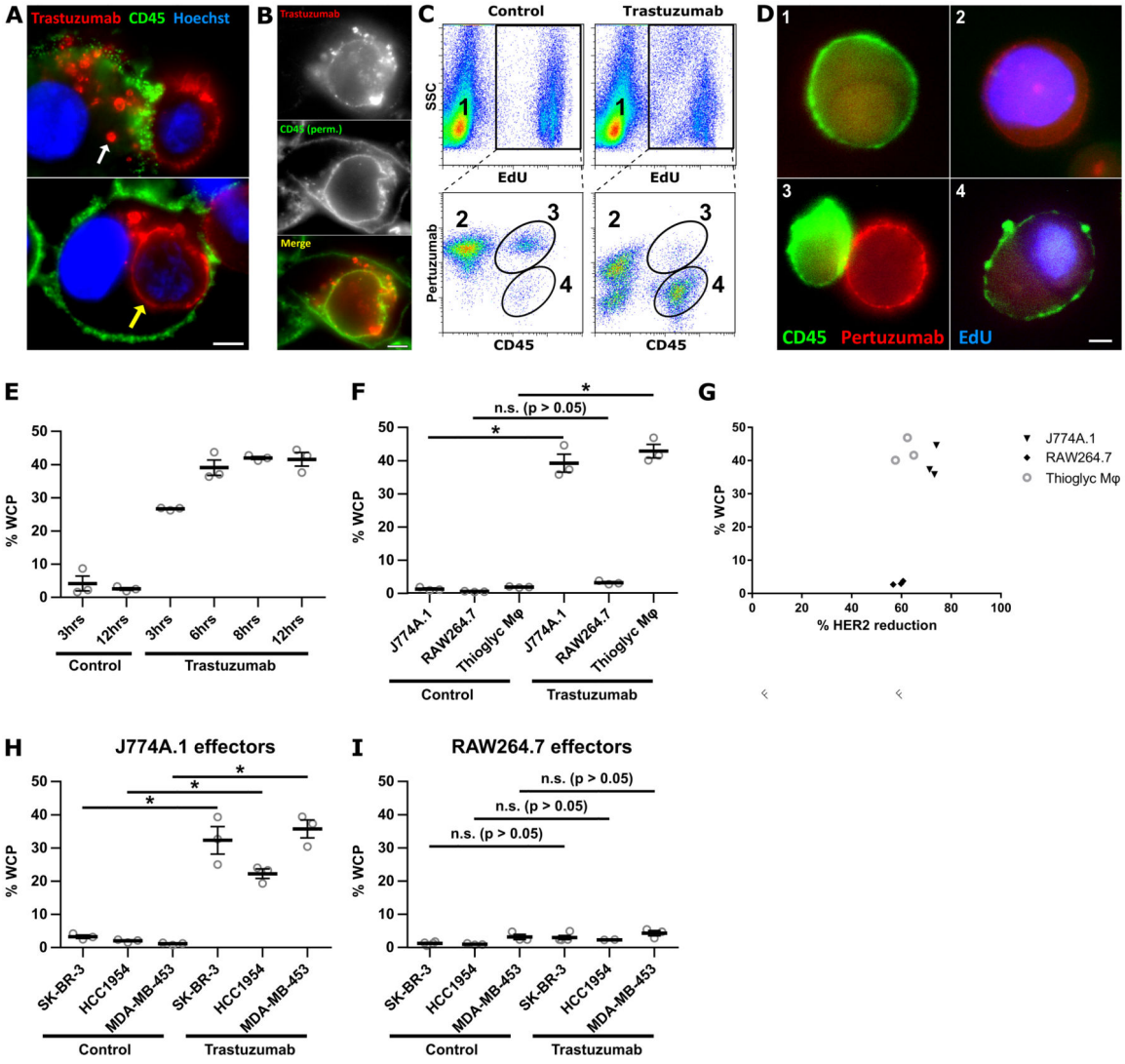

Figure 2.

J774A.1 and RAW264.7 macrophages exhibit different phagocytic activities. **A**, MDA-MB-453 cells were harvested and opsonized by incubation with 10 μg/ml Alexa 555-labeled trastuzumab at room temperature for ten minutes followed by washing. The opsonized cancer cells (2.5×10^4 cells/imaging dish) were added to adhered, IFNγ-activated J774A.1 macrophages (4×10^4 cells) for 30 minutes and the samples fixed and stained. Trogosomes and a completely engulfed cancer cell are indicated by white and yellow arrows, respectively. **B**, J774A.1 macrophages and MDA-MB-453 cells were incubated as in **A**, fixed, permeabilized and mouse CD45 detected using FITC-labeled mouse CD45-specific antibody. **C**, representative flow cytometry plots to show the identification of the whole cell phagocytosis (WCP) population. Macrophages were plated for 18 hours, followed by addition of EdU-treated cancer cells at a 10:1 effector:target cell ratio in the presence of 1 μg/ml trastuzumab or PBS vehicle for 6 hours. The samples were then harvested and stained for mouse CD45 (macrophages) and cancer cells accessible to the medium were detected using labeled pertuzumab. The following cell populations can be identified: macrophage

only (1); cancer cell only (2); macrophage:cancer cell conjugate (3); macrophage that has performed WCP (4). **D,** fluorescence microscopy images of cells representative of the populations numbered 1, 2, 3 and 4 in panel **C**. **E**, time-course of WCP using J774A.1 macrophages and MDA-MB-453 cancer cells. **F**, comparison of WCP activity using different macrophage cells with MDA-MB-453 cells after co-incubation for 6 hours. **G,** plot of percentage WCP against percentage HER2 reduction for the data shown in Fig. 2F. The percentage of HER2 reduction from the cell surface was calculated from the ratio of the surface pertuzumab (MFI) remaining in the non-phagocytosed cancer cell population to surface pertuzumab (MFI) in samples without antibody treatment. **H,I**, comparison of WCP activity using J774A.1 (**H**) or RAW264.7 (**I**) macrophages with different breast cancer cell lines after co-incubation for 6 hours. Control in panels **C, E-I**, represent co-cultures incubated without trastuzumab. Error bars represent standard errors. Student's *t*-test was performed to indicate statistical significance (denoted by *; $p < 0.05$). n.s., no significant difference ($p>0.05$). For panels **A, B** and **D**, scale bars = 5 μm.

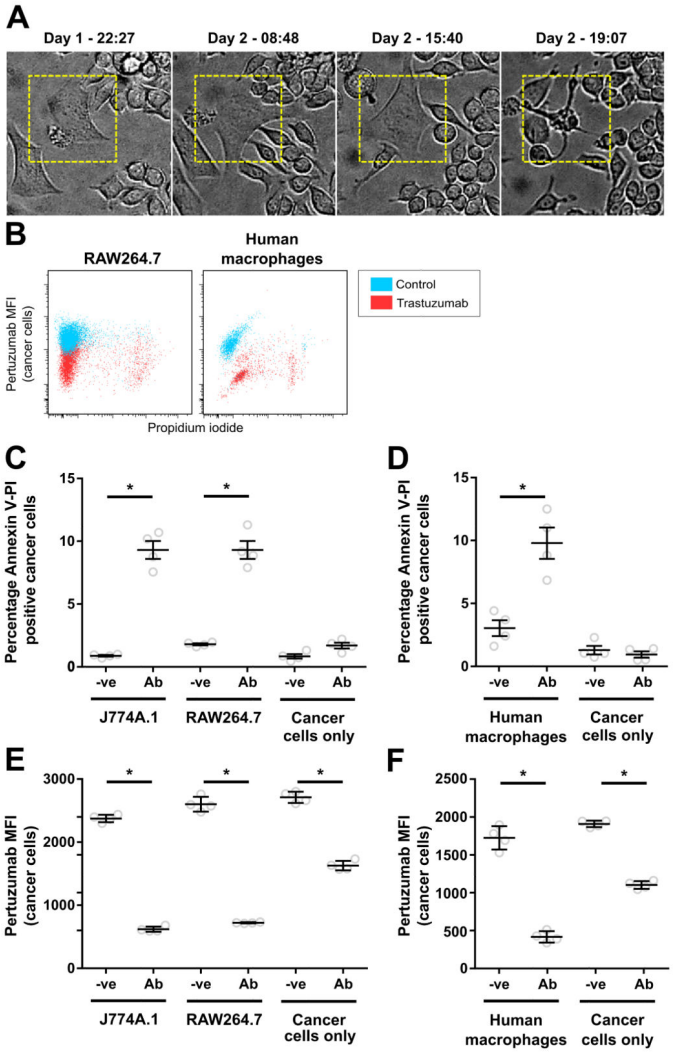

Figure 3.

RAW264.7, J774A.1 and human monocyte-derived macrophages induce similar levels of apoptosis in opsonized cancer cells. Macrophages and cancer cells were plated at an effector:target cell ratio of 4:1 in a T25 culture flask (3×10^6:7.5×10^5 cells), 1 μg/ml trastuzumab was added 18-24 hours later and the cells were imaged. **A**, individual frames showing an SK-BR-3 cell undergoing cell death in a long-term light microscopy imaging experiment for a co-culture of SK-BR-3 and RAW264.7 cells in the presence of 1 μg/ml trastuzumab. Times of acquisition of each image are indicated. **B,C**,**D,** MDA-MB-453 cells were plated alone or co-incubated with RAW264.7, J774A.1 or human monocyte-derived macrophages at a 4:1 effector:target cell ratio in the presence of 1 μg/ml trastuzumab (Ab) or PBS vehicle (-ve) for 36 hours. **B**, representative dot-plots for pertuzumab fluorescence vs. PI fluoresence for cancer cells from co-cultures of RAW264.7 or human macrophages with cancer cells in the presence (trastuzumab) and absence of antibody (control). **C,D,** fraction of annexin V, PI double-positive cancer cells in co-cultures determined by flow cytometry. **E,F,** samples shown in C and D, respectively, were stained with fluorescently labeled pertuzumab after harvesting and the mean fluorescent intensity (MFI) of pertuzumab on the

cancer cell populations determined. Error bars represent standard errors. Student's *t*-test was performed to indicate statistical significance (denoted by *; $p < 0.05$).

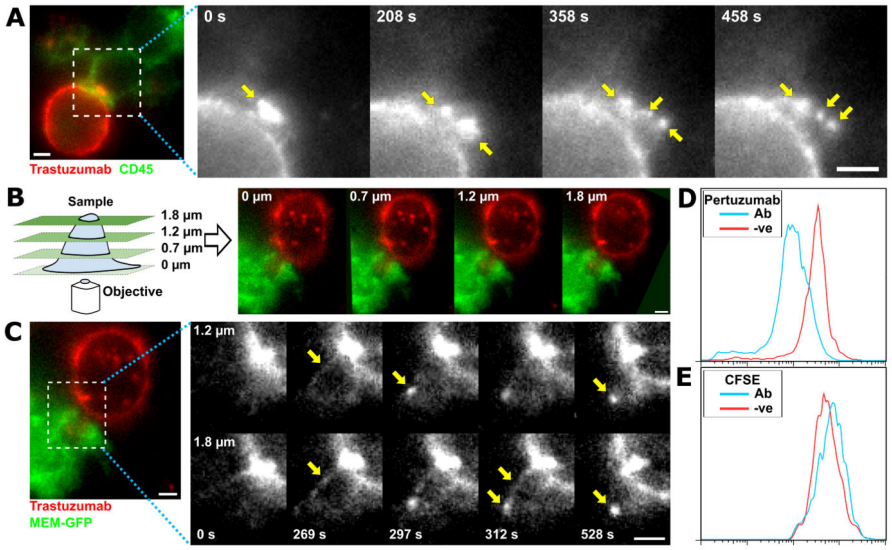

Figure 4.

Fluorescence microscopy analyses using MUM reveals that trogocytosis involves tubular extensions of the cancer cells. **A,** individual frames from a live imaging experiment of MDA-MB-453: RAW264.7 cell conjugates. The cancer cells were opsonized by incubation with 10 μg/ml Alexa 555-labeled trastuzumab at room temperature for ten minutes followed by washing. These cells were added to IFN-γ-activated RAW264.7 macrophages expressing MEM-GFP (to label the plasma membrane; pseudocolored green) plated in dishes 30 minutes prior to imaging at a 1:1 effector:target cell ratio (2.5×10^4 cells). Grayscale images represent individual frames of the trastuzumab signal for the boxed region in the pseudo-colored image showing trastuzumab (red) and MEM-GFP (green) signals. Yellow arrows indicate punctate structures accumulating inside the macrophage. **B**, schematic diagram of the MUM configuration and representative images from multiple focal planes of a macrophage:cancer cell conjugate formed between IFN-γ-activated MEM-GFP expressing RAW264.7 macrophages and MDA-MB-453 cancer cells opsonized with Alexa 555-labeled trastuzumab as above. **C**, individual frames showing the trastuzumab signal (black and white panels) of live cell imaging from two focal planes displaying a trogocytic event involving tubulation. Yellow arrows indicate intermediates in the tubulation process. Numbers in the lower part of each panel represent the acquisition time (seconds) for each image pair. The left panel shows an overlay of the MEM-GFP (pseudocolored green) and trastuzumab (pseudocolored red) at 1020 sec in the 1.8 μm focal plane. The boxed region is expanded in the grayscale images. **D, E**, flow cytometry analyses of pertuzumab and CFSE staining levels in MDA-MB-453 cells co-incubated with RAW264.7 macrophages as described in Fig. 1B. Scale bars = 5 μm.

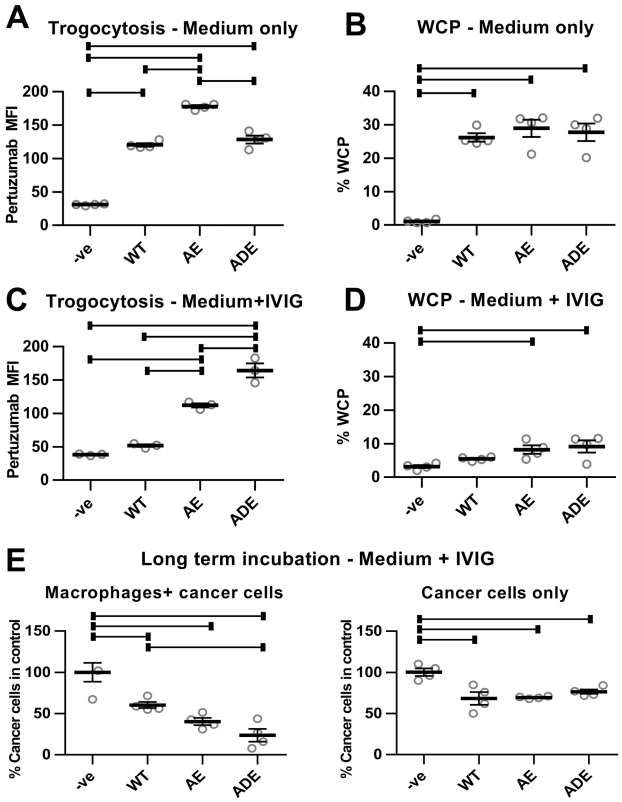

Figure 5.

Antibodies with enhanced affinity for activating FcγRs have increased trogocytic and cell-killing activity. **A,** thioglycollate-elicited macrophages isolated from C57BL/6 mice transgenically expressing human FcγRs (hFcγR macrophages; 26) were plated with MDA-MB-453 cells at an effector:target ratio of 0.4:1 (4×10^4:1×10^5 cells). 18 hours later, 1 μg/ml wild type (WT) trastuzumab or engineered trastuzumab variants with enhanced affinity for FcγRIIa and FcγRIIIa (AE and ADE), combined with 0.5 μg/ml Alexa 488-labeled Fab fragments derived from pertuzumab, were added to the co-cultures for 60 minutes. As controls, cells were also co-cultured without trastuzumab (-ve). The mean fluorescence intensity (MFI) values for pertuzumab Fab staining in the macrophage population are shown. **B,** WCP assay was performed as before using hFcγR macrophages plated for 18 hours, followed by addition of 10-fold lower numbers of cancer cells and 10 μg/ml WT, AE or ADE trastuzumab variants for 6 hours. Trogocytosis (**C**) and WCP (**D**) assays were performed as in **A,B**, but in the presence of 10 mg/ml IVIG. Under the conditions of the trogocytosis assays (60 minutes incubation), phagocytosis of cancer cells was at background, control levels (data not shown). **E,** hFcγR macrophages were plated with cancer cells at an effector:target cell ratio of 2:1 (5×10^4:2.5×10^4 cells) or cancer cells alone for 24 hours, followed by addition of 10 mg/ml IVIG and 10 μg/ml WT, AE or ADE variants of trastuzumab. The medium was replaced by new medium containing the same additions after 3 days. Cells were harvested after 5 days and the remaining numbers of cancer cells quantitated. Error bars represent standard errors. For **A-E**, one-way ANOVA analyses were carried out followed by a Tukey's multiple comparisons test between all sample pairs with a

confidence interval of 95%. Horizontal lines indicate significant differences between sample pairs.